

Persistent room-temperature relaxation of InP amorphized and compacted by MeV ion beams

L. Cliche and S. Roorda

Groupe de recherche en physique et technologie des Couches-Minces, Département de Physique, Université de Montréal C.P. 6128 succ. centre-ville, Montréal, Québec H3C 3J7, Canada

R. A. Masut

Groupe de recherche en physique et technologie des Couches Minces, Département de Génie Physique, École polytechnique de Montréal, C. P. 6079 succ. centre-ville, Montréal, Québec H3C 3A7, Canada

(Received 11 April 1994; accepted for publication 24 July 1994)

Ion beam induced deformation and compaction has been observed in InP, amorphized by MeV Se ion implantation. The initial density of amorphous InP is $0.55\% \pm 0.05\%$ larger than that of crystalline InP. During a period of two months, most of the excess density is lost in a spontaneous, room-temperature relaxation. This relaxation can be described by two time constants: $\tau_1 \approx 8 \pm 2$ h and $\tau_2 \approx 14 \pm 1$ days. © 1994 American Institute of Physics.

Most crystalline semiconductors expand when subjected to ion bombardment. This is true in the low fluence regime, where the ion beam damage consists of point defects and small defect clusters¹⁻³ as well as in the high fluence regime, where the material has been amorphized.^{4,5} In the case of amorphous Si and Ge, the new phase is known to exhibit structural relaxation which lowers its Gibbs free energy.^{6,7} This relaxation occurs at temperatures as low as 77 K,⁸ with a time constant of several minutes irrespective of temperature.^{7,8} During the relaxation, the density remains essentially unchanged.⁴ Since both the ion beam induced expansion and the structural relaxation are quite common in pure and alloyed semiconductors, one might suspect that InP shows similar behavior. This is, however, not so. It is known that in the low-fluence regime, InP contracts.² We now show that amorphous InP is more dense than crystalline InP and, moreover, that a room-temperature structural relaxation occurs, persisting for several months, continually changing the density.

Semi-insulating InP (100) wafers were degreased and clamped to a copper block, using vacuum grease for improved thermal contact. They were then implanted at room temperature with 10^{14} cm⁻² Se ions at several energies (see Table I), with low beam current, limiting the areal power density to less than 0.6 W/cm². Alternating stripes of amorphous/crystalline InP were produced by using a steel contact mask placed directly on the sample. The implantations were carried out in a vacuum of 4×10^{-8} mbar. After implantation, the surface was profiled with a stylus profilometer (DEKTAK 3030 ST). Each surface profile of 8 mm of the masked surface covered 10 periods of alternating amorphous/crystalline material. We have repeated the measurements several times over a period of 70 days following implantation. During that time, one sample was kept at liquid nitrogen temperature and all the others were left at room temperature. Successive profiles were taken at the same place on the samples and with the same applied stylus force (0.05 mN). The curvature of each sample was determined using a polynomial fit, and subtracted from the data to yield a corrected profile. The *c*-InP/*a*-InP step was measured on the corrected profiles and each reported value is the average

of twenty individual steps with the error being the standard deviation. Some unmasked samples were chemically bevelled in a solution of bromine:methanol(1:19). The bevels were made deep enough to reach the substrate under the amorphized layer. Again with a profilometer, we measured the thickness of the amorphous layer by measuring the depth of the bevel at the amorphous/crystalline interface.

Some examples of surface profiles are shown in Fig. 1. The dashed line is the surface profile of the InP prior to the implantation. It shows that the sample is not flat, but curved with an initial radius of curvature *R* of 16 m. The surface profile after ion implantation (see Table I, sample #1) is shown as a solid line. Two clear differences can immediately be observed relative to the unimplanted case: first, the ion implanted sample has a stronger curvature (*R*=6.1 m) and second, a series of depressed regions is seen. These regions correspond to the amorphous stripes and are indicative of a compaction of the InP upon amorphization. The dash-dotted line shows the corrected data obtained by subtracting a polynomial fit representing the curvature of the sample. For this profile, which was taken immediately after amorphization, the average step height was determined to be 55 ± 2 nm. With the low fluence needed to amorphize the material (7×10^{14} ions/cm² at most), both the added material and the estimated amount of sputtered material⁹ were negligible. Therefore, the step height is a direct measure of the vertical deformation.

The depression of the implanted surface suggests that there is a compaction of the implanted material. However, we observe bending of the sample away from the implanted surface. Compaction should bend the wafer towards the surface [see Fig. 2(a)] and not in the opposite direction as is observed here. A curvature away from the implanted surface would be observed if the in-plane dimension of the implanted material increases. This effect has been described as

TABLE I. Ion implantation parameters and amorphous layer thickness.

Sample	Implantation energies (MeV)	<i>d</i> (μm)
1	2, 3.6, 6, 10, 17, 24, 30	8.0 ± 0.5
2	2, 3.6, 6, 10	4.2 ± 0.4

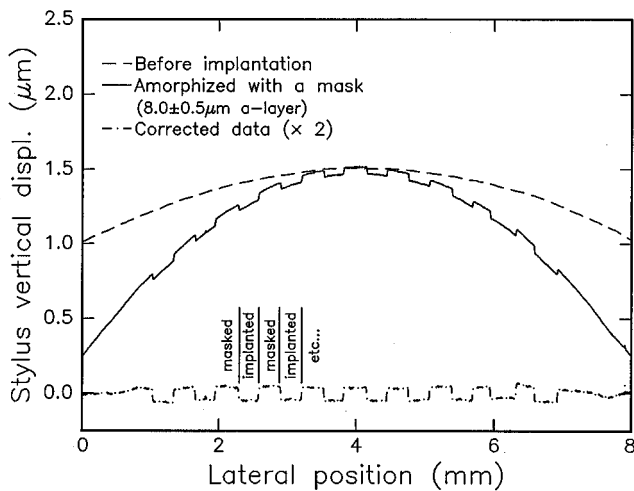


FIG. 1. Surface profile of the InP prior to the implantation (dashed line) and after implantation through a mask (solid line). Also shown is the corrected profile (dot-dashed) obtained by subtracting a polynomial fit of the residual curvature of the sample (multiplied by 2 for clarity).

a hammering effect¹⁰ [see Fig. 2(b)]. In order to properly interpret the data, we have to compare quantitatively the vertical deformation, which is measured directly by the step height, and the horizontal deformation, which can be estimated from the measured curvature using elasticity theory. When the implanted surface regions expand horizontally, a compressive stress accumulates in the wafer. The wafer will slightly bend and deform so as to reduce the deformation of the *a*-InP regions. Minimizing the total elastic energy of the system leads to a relation between the strain reduction in the *a*-InP regions ΔL , resulting from the deformation of the substrate, and the radius of curvature R of the wafer:¹¹

$$\frac{\Delta L}{L_s} = \frac{2t_s}{3R}. \quad (1)$$

Here, L_s is the arc length, or the wafer length, and t_s is the thickness of the wafer. Formula (1) is valid when t_s is much larger than the thickness of the amorphous layer. We evaluated for four different samples $\Delta L/L$, where L is the width of the *a*-InP fingers, and compared it to $\Delta d/d$, the vertical

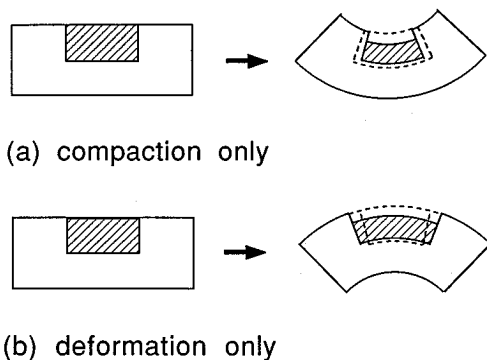


FIG. 2. Schematic representation of wafer curvature due to thin film (a) compaction, or (b) deformation. Not to scale.

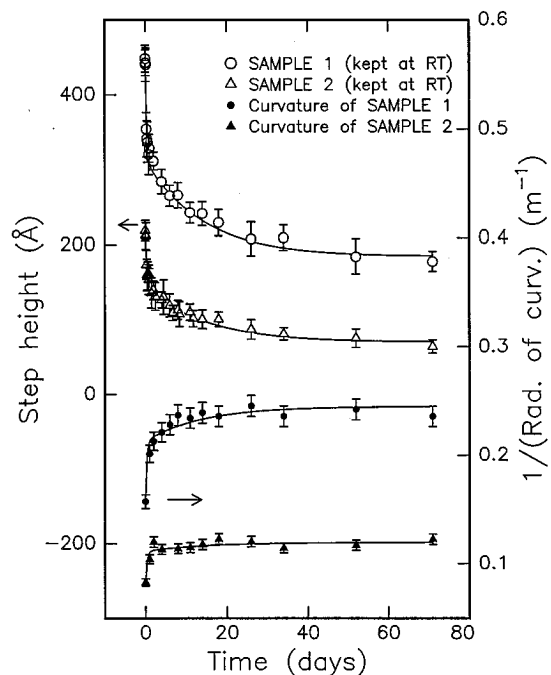


FIG. 3. Time evolution of step height (top two curves) and curvature (bottom two curves). The full line is a double exponential fit with $\tau_1=8$ h and $\tau_2=14$ days.

change. We found that the horizontal deformation $\Delta L/L$ is at most 4% of the vertical deformation $\Delta d/d$ and whence the depression shown in Fig. 1 is mostly due to compaction. The ratio of the crystalline and amorphous densities can then be calculated from

$$\frac{\delta_a}{\delta_c} = \frac{1}{1 - (\Delta d/d) + (2\Delta L/L)}, \quad (2)$$

where we omit higher order terms. Immediately after implantation, the larger value of $2\Delta L/L$ observed is 0.01% (for sample 1) and the averaged $\Delta d/d$ is 0.56%. At that point we find that the density of *a*-InP is $0.55 \pm 0.05\%$ larger than that of *c*-InP.

Figure 3 shows the variation of the average step height and curvature over a period of more than two months for two different samples. The step height decreases with time and appears to saturate after several months. At the same time, the curvature of the implanted samples increases in such a way that a linear relation between the increase of the curvature and the decrease of the step height could be observed. The variation of the step height and the curvature was stopped on a sample which was kept at liquid nitrogen temperature. After 70 days, the density of *a*-InP has decreased and we find from relation (2) that it is $0.17\% \pm 0.06\%$ larger than that of *c*-InP.

The step height and curvature data both exhibit an initially fast change followed by a long tail, and could not be described by a single time constant. A double exponential was used to fit the data as shown in Fig. 3 (solid lines). We were able to fit all the data, within the experimental errors, with the same two time constants; a fast initial recovery time

constant $\tau_1 \approx 8 \pm 2$ h and a slower recovery $\tau_2 \approx 14 \pm 1$ days. This shows that the increase of the curvature and the step height recovery have similar kinetics.

In the case of Si, structural relaxation of the amorphous phase has been shown to be closely related to defect annealing in the crystalline phase.⁷ In the light of this similarity, it is interesting to compare our observation of the persistent relaxation of amorphous InP with the behavior of ion beam damaged crystalline InP. Indeed, a spontaneous recovery at room temperature has been observed in crystalline InP containing a distribution of point defects.^{12,13} In one experiment,¹² InP had been implanted with 0.6 MeV Si ions. For fluences less than $4 \times 10^{13} \text{ cm}^{-2}$ (the critical fluence for amorphization), a spontaneous recovery could be observed. Like our data shown in Fig. 3, that recovery exhibited two time constants. However, the time constants were much longer than the ones observed in amorphous InP. ($\tau_1 < 5$ days and $\tau_2 \approx 100$ days, to be compared with $\tau_1 = 8$ h and $\tau_2 = 14$ days). It remains to be established whether this reflects a difference in kinetics intrinsic to amorphous and crystalline InP or a difference in storage temperature.

Density variations during relaxation have also been observed in *a*-Si. The *a*-Si first expands by 0.1% during heating from room temperature to 250 °C and then densifies on further heating.¹⁴ The fact that both *a*-Si and *a*-InP expand during the initial anneal stages may indicate that in both cases a preferential annealing of excess density (i.e., interstitial type) defects occurs. This is somewhat surprising since the density change associated with amorphization has opposite sign: Si expands while InP compacts when amorphized.

In conclusion, InP can be macroscopically deformed and compacted by ion beam induced amorphization. Immediately after the implantation, we observed an increase of the in-plane dimension of the material and an out of plane compac-

tion. The vertical dimensional change is mostly due to an overall compaction and the initial density of *a*-InP is larger than that of *c*-InP by $0.55\% \pm 0.05\%$. When kept at room temperature, a spontaneous annealing process occurs which is characterized by two time constants, namely $\tau_1 = 8 \pm 2$ h and $\tau_2 = 14 \pm 1$ days.

It is a pleasure to acknowledge the expert assistance of P. Bérichon and R. Gosselin with the operation of the tandem accelerator, R. Arès who set up the bevel preparation technique, and M. Verhaegen who did some of the profilometry. This work is financially supported by the Natural Science and Engineering Research Council of Canada (NSERC) and the Fonds pour la Formation de Chercheurs et l'Aide à la Recherche (FCAR).

¹F. L. Vook, Phys. Rev. **125**, 855 (1962).

²C. R. Wie, T. Jones, T. A. Tombrello, T. Vreeland, Jr., F. Xiong, Z. Zhu, G. Burns, and F. H. Dacol, Mater. Res. Soc. Symp. Proc. **74**, 517 (1987).

³Y. B. Trudeau, R. Arès, G. E. Kajrys, G. Gagnon, M. Jouanne, and J. L. Brebner, Nucl. Instrum. Methods B **80/81**, 706 (1993).

⁴J. S. Custer, M. O. Thompson, D. C. Jacobson, J. M. Poate, S. Roorda, W. C. Sinke, and F. Spaepen, Appl. Phys. Lett. **64**, 437 (1994).

⁵K. Laaziri, S. Roorda and L. Cliche, Nucl. Instrum. Methods B **90**, 438 (1994).

⁶E. P. Donovan, F. Spaepen, and D. Turnbull, J. Appl. Phys. **57**, 1795 (1985).

⁷S. Roorda, W. C. Sinke, J. M. Poate, D. C. Jacobson, S. Dierker, B. S. Dennis, D. J. Eaglesham, F. Spaepen, and P. Fuoss, Phys. Rev. B **44**, 3702 (1991).

⁸S. Coffa, F. Priolo, and A. Battaglia, Phys. Rev. Lett. **70**, 3756 (1993).

⁹P. Sigmund, Phys. Rev. **184**, 383 (1969).

¹⁰S. Klaumünzer, M. Rammensee, S. Löffler, and H. C. Neitzert, J. Mater. Res. **6**, 2109 (1991).

¹¹P. A. Flinn, D. S. Gardner, and W. D. Nix, IEEE Trans. Electron Dev. **ED-34**, 689 (1987).

¹²U. G. Akano, I. V. Mitchell, and F. R. Shepherd, Appl. Phys. Lett. **59**, 2570 (1991).

¹³E. F. Kennedy, Appl. Phys. Lett. **38**, 375 (1980).

¹⁴C. A. Volkert, J. Appl. Phys. **74**, 7107 (1993).